Macromolecules

Article

pubs.acs.org/Macromolecules

Characterization of Network Structure and Chain Dynamics of Elastomeric Ionomers by Means of ^{1}H Low-Field NMR

M. A. Malmierca,*[,†] A. González-Jiménez,[†] I. Mora-Barrantes,[†] P. Posadas,[†] A. Rodríguez,[†] L. Ibarra,[†] A. Nogales,[‡] K. Saalwächter,*[,§] and J. L. Valentín*[,†]

[†]Instituto de Ciencia y Tecnología de Polímeros (CSIC), C/Juan de la Cierva, 3, 28006 Madrid, Spain

[‡]Instituto de Estructura de la Materia, IEM-CSIC, C/Serrano 121, 28006 Madrid, Spain

[§]Institut für Physik − NMR, Martin-Luther-Universität Halle-Wittenberg, Betty-Heimann-Strasse 7, D-06120 Halle, Germany

Supporting Information

ABSTRACT: The network structure and chain dynamics of ionic elastomers based on carboxylated nitrile rubber (XNBR) cross-linked with different content of magnesium oxide (MgO) have been studied by different low-field time-domain NMR experiments. Ionic contacts created during the vulcanization tend to aggregate trapping some polymer segments that show restricted mobility as it was quantified by analyses of refocused free induction decays. Increasing the MgO content above the stoichiometric fraction has no effect on the amount of trapped polymer segments, but it increases the network cross-link density as measured by multiple-quantum (MQ) NMR experiments. The central finding of this work is that MgO addition above the stoichiometric content enhances the mechanical properties by creating a larger number of smaller ionic clusters, which act as dynamic cross-links, but are not readily seen by other techniques. Changes in the network structure and morphology of segregated thermolabile ionic domains have an impact on the ionic rearrangement dynamics and, in consequence, on the thermoplastic behavior of these materials at elevated temperatures.

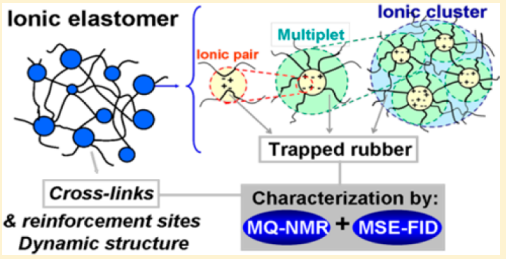

INTRODUCTION

Elastomers are polymers characterized by a long-range elasticity obtained after the vulcanization process (mainly via with sulfur or organic peroxides) because of the creation of covalent cross-links between chains.[1−4] The nature of these cross-links is permanent and irreversible, and consequently, most of the elastomers present recycling problems. In order to overcome this disadvantage, thermoplastic elastomers have been developed,[5,6] and ionic elastomers are among these candidates owing to the thermolabile nature of ionic associations.[7]

Ionic elastomers contain a relatively small number of ionic groups (e.g., carboxylic, sulfonic, etc.), either pendant to or incorporated in the nonpolar main chains. These groups are usually neutralized with metal cations forming ion pairs, which constitute the simplest form of inter- or intrachain interaction. They tend to aggregate into more complex structures, i.e., multiplets of different sizes,[8] according to the ion content, nature, and size of the polyion and counterion, dielectric constant of the matrix polymer, T_g of the polymer, rigidity of the backbone, position of the ion pair relative to the backbone, steric constraints, amount and nature of added plasticizers, presence of added fillers, etc.[9−11] In those multiplets, the polymer segments closer to the ionic groups are firmly attached by the strong electrostatic interactions. This fact reduces the chain mobility[12,13] in comparison with the bulk polymer, and in consequence, a mobility gradient should be observed according to the distance from the multiplet surface. In some cases multiplets, or more precisely the polymer layers with restricted mobility that surround the multiplets, can overlap forming larger aggregates named clusters. In this case, ionomers show phase-separated morphology, which is composed by ion-rich nanodomains surrounded by highly restricted polymer areas, characterized by its own thermal transition, the so-called ionic transition.[8]

Although there is no consensus yet in the description of the morphology and structure of ionic aggregates,[8,14−21] it is qualitatively clear that the complex hierarchical structure of ionic contacts acts as cross-links and a reinforcing point, thus generating a polymer network with unique elastic properties.[22−24]

Extensive investigations were focused on the structure characterization of ionic aggregates and the ionomer morphology by using X-ray scattering,[17,19,25] transmission electron microscopy (TEM),[26−29] and dynamic mechanical analysis (DMA).[16,30,31] However, the basic knowledge about the network structure and chain dynamics is still insufficient in order to understand the exceptional elastic properties of these complex materials.

In this sense, time-domain solid-state NMR spectroscopy has emerged as a versatile, powerful, and successful tool to

Received: June 11, 2014
Revised: August 4, 2014
Published: August 18, 2014

investigate those factors in different rubber materials.[32−38] However, this experimental approach has not been widely applied to characterize elastomeric ionomers. In previous attempts,[18,21] the Hahn-echo pulse sequence was used to record the (long-time) transverse relaxation (T_2) behavior of the *mobile* part of the bulk polymer, which reflects the segmental dynamics and conformational restrictions in the polymer chains imposed by the formation of ionic cross-links, i.e., the rubber network structure. As a complement, the solid-echo pulse sequence was applied to analyze the *rigid* polymer fraction around the ionic aggregates exhibiting rather short T_2, which reflects its restricted mobility and slower dynamics.[12,13]

Relaxation experiments are based on the study of the NMR line width, which is dipolar in origin, in the form of an apparent second moment $\sim 1/T_2$.[39,40] However, the quantitative analysis of the relaxation curves has been criticized because of the overinterpreted fitting models with parameter interdependencies.[41,42] Thus, other NMR methods which make a more direct use of the dipolar couplings as the main origin of the measured phenomena seem to represent a more reliable alternative.[38,43]

In the past years, multiple-quantum (MQ) NMR experiments have been intensively used to provide absolute-scale information on the local dynamic chain order parameter, which is related to restrictions of the collective chain motions (e.g., slow relaxation processes in the range of 0.1−3 ms) caused by the presence of cross-links and/or topological constraints.[33,34,37,44] In the high-temperature regime, the data from MQ experiments can be processed in such a way that the temperature-independent network structure effect can be separated from the temperature-dependent segmental dynamics without invoking any specific model. In consequence, this approach provides a more precise quantification of the cross-link density and their spatial distribution than the widely used Hahn echo experiments.

In addition, the magic sandwich echo (MSE) sequence can be used to more quantitatively refocus the free induction decay (FID) signal in cases where the signal decay reaches the time scale of the instrumental dead time.[45−47] The analysis of the so-obtained FIDs is thus a complementary method to characterize the polymer fraction with stronger dipole−dipole interactions and hence faster relaxation behavior (less than 0.2 ms).

The main objective of the present work is to investigate the network structure and chain dynamics of ionic elastomers and their evolution with the temperature, using the most current and reliable time-domain NMR approaches. These methodologies, performed in an inexpensive and easy-to-use low-field spectrometer, provide new insights into the structure−dynamics−property relationships, which are the key to understand the unique properties of these materials.

EXPERIMENTAL SECTION

Materials and Preparation of Samples. Carboxylated nitrile rubber (XNBR) was supplied by Lanxess Elastomers SAS (Germany) under the trade name of Krynac X740. It contains 26.5 wt % acrylonitrile and 7 wt % carboxylic groups (−COOH) according to the manufacturer. The vulcanization system was based on magnesium oxide (MgO, supplied by Akrochem with the trademark Elastomag 170 Special) to create ionic cross-links. Compounds contain 1 part per hundred of rubber (phr) of stearic acid and increasing proportions of magnesium oxide: 1, 2, 3.26, 4, 6, 8, and 12 phr, where 3.26 phr is the stoichiometric concentration to neutralize the carboxylic acid groups. Covalent networks (obtained by addition of 1 phr of stearic acid and 2 or 4 phr of dicumyl peroxide, DCP) were prepared to be compared with the ionic samples. In this article, the name of samples, e.g. MgO-4, indicates the vulcanizing agent, MgO or DCP, and their amount (in phr).

Compounds were prepared on a Gumix laboratory two-roll mill with a cylinder diameter of 15 cm and a length of 30 cm and a friction ratio of 1:1.15. The rolls were kept cold during the mixing procedure by circulating cold water through them. Vulcanization curves were obtained in a rubber process analyzer RPA 2000 (Alpha Technologies) with a deformation of 6.98% and an oscillatory frequency of 1.667 Hz. The vulcanization was carried out in a hydraulic press at 160 °C during a fixed time of 120 min for ionic systems.[48] Covalent samples (DCP-2 and DCP-4) were vulcanized 35 and 20 min, respectively, according to their optimum vulcanization times (t_{99}) deduced from their rheometer curves at 160 °C.

Rheometric Measurements. Different rheometric measurements were performed in a rubber process analyzer RPA 2000: (a) Frequency-sweep experiments were carried out after the vulcanization process. The shear modulus was measured at frequencies from 0.002 to 33.33 Hz at temperatures from 40 to 230 °C. Using the frequency−temperature superposition,[49] a combined master curve was plotted to obtain the stress relaxation of the modulus in a wide range of frequencies. (b) The Payne effect was evaluated on vulcanized samples at different temperatures by measuring the storage modulus (G') at different shear strain amplitudes. (c) Besides the vulcanization curves, the elastic torque was acquired at different temperatures maintaining the deformation (6.98%) and oscillatory frequency (1.667 Hz). A delay time of 10 min was required to achieve the correct temperature. After that, elastic torque was recorded during 15 min.

Dynamic Mechanical Thermal Analysis (DMTA). Dynamic mechanical measurements of vulcanized samples were carried out in a Rheometric Scientific DMTA V dynamic mechanical thermal analyzer working according to standard ISO 6721 in the tensile mode at frequency of 1 Hz and a strain around 0.05%, which is in the linear regime. The temperature was varied from −60 to 200 °C at a rate of 1.5 K/min. Each specimen was cut out into a rectangular strip with approximate dimensions 30 × 6 × 2 mm^3.

NMR Spectroscopy. Time-domain ^{1}H NMR measurements were performed on a low-field Bruker Minispec mq20 spectrometer at 20 MHz proton resonance frequency (0.5 T) with 90° pulses of 3 μs length and a dead time of 12 μs. The sample temperature was controlled with a BVT3000 heater working with air. In order to avoid degradation, samples were flame-sealed in 8 mm NMR tubes under vacuum conditions. Two approaches, e.g. multiple-quantum (MQ) and magic sandwich echo (MSE) experiments, were used in order to characterize the complex structure of these materials.

Multiple-Quantum (MQ) Spectroscopy. MQ NMR has been found to be the most reliable NMR tool for the analysis of network structure in elastomers.[33,50] The usual procedure for these experiments is explained in the Supporting Information (see Figures S1 and S2). This measurable effect relies on the orientation dependence of the (fluctuating) dipolar coupling tensor with respect to the magnetic field, which can be described by an orientation autocorrelation function (OACF) of the chain segments.[37,51] At short times (fast segmental dynamics, in the range of nanoseconds to microseconds) the OACF of the polymer segments decays quickly due to the fast local fluctuations between the accessible spatial conformations, until it reaches a plateau value in the case of polymer networks (independently of the nature of cross-links[34,52,53]). In that region, the measurable weak residual dipolar couplings, D_{res}, is directly proportional to a local dynamic order parameter of the polymer backbone S_b, giving information about the network structure:[33]

$$S_b = k\frac{D_{res}}{D_{stat}} = \frac{3}{5}\frac{r^2}{N} \quad (1)$$

Here, k is a parameter that represents the local coupling topology and intrasegmental motions that should be used to rescale the static coupling constant, D_{stat} (determined by the fixed proton−proton distances), in order to account for averaging effects that occur on the level below the segmental (Kuhn) length, r^2 is the ratio of the end-to-

dx.doi.org/10.1021/ma501208g | Macromolecules 2014, 47, 5655−5667

end vector to its average unperturbed melt state, and N represents the number of statistical (Kuhn) segments between constraints.

According to these statements, temperature plays a central role in MQ measurements. It is required to be far above the polymer glass-transition temperature (T_g) to be sure that the segmental dynamics is fast enough to sweep out the whole conformational space between constraints, achieve full averaging, and consequently avoid the overestimation on the cross-link density.[54,55] In case of elastomeric ionomers, the structure changes with temperature, and it is an additional challenge to determine the lowest temperature to achieve physically meaningful results by NMR. To address that problem, the matrix (XNBR) was vulcanized with different amounts of dicumyl peroxide (from 0.25 to 2 phr) in order to create covalent cross-links. Such thermostable networks always show lower cross-link density than ionomers,[48] and they reach a clear plateau at temperatures close to 80 °C (see Supporting Information, Figure S3). It means that polymer dynamics at 80 °C is fast enough to average out all the segmental conformations in the NMR time window for all studied samples. According to these statements, MQ-NMR measurements at 80 °C provide the more reliable information about the cross-link density in ionomers, whereas the information extracted at higher temperatures will address the evolution of that initial network structure because of the dynamic nature of ionic interactions, as it will be widely explained in the following sections.

In addition, the application of the standard MQ pulse sequences (based upon a clean double-quantum Hamiltonian[56]) and the well-described analysis procedure[33] is inappropriate to the study of elastomeric ionomers as it will be demonstrated in the Results section. The coexistence of rubber segments with quite different dynamics requires a new strategy to characterize the network structure of these samples by using a combination of different MQ NMR experiments.

Magic Sandwich Echo (MSE)-FID. The MSE is used to overcome the dead time problem in the acquisition of FIDs. This is a negligible issue in weakly dipolar-coupled samples, e.g. rubber matrices, characterized by long transverse relaxation times. However, it is a central issue in order to quantify the fraction of protons in rigid environments with restricted mobility because their NMR signal relaxes before the beginning of acquisition (<12 μs in the case of the used spectrometer). Compared with a solid echo, the MSE enables a better refocusing of multispin dipolar interactions and has been shown to be a robust method to investigate polymer mobility.[46,47] These NMR experiments were performed with a pulse sequence detailed elsewhere[46] at different temperatures (from 40 to 160 °C) in order to investigate the evolution of trapped polymer domains in elastomeric ionomers. Analysis details applied to take into account the special properties of elastomeric ionomers based on an XNBR matrix will be described in the Results section.

Mechanical Properties. Tensile tests were performed in an Instron model 3365 dynamometer equipped with a video camera to measure deformations at a strain rate of 500 mm/min on type 2 dumbbell samples, according to UNE-ISO 37:2011 standard. Five specimens were tested for each sample. Tearing tests were carried out on angular-type samples, in accordance with the UNE-ISO 34-1:2011, at the same deformation rate used for tensile tests. Three specimens were tested for each sample. The abrasion resistance was determined according to national standard UNE 53527:1991. Three specimens were tested for each sample. Compression set values were obtained following the UNE-ISO 815-1:2011 standard protocol. Three specimens were tested for each sample at 70 °C and at room temperature.

EXPERIMENTAL RESULTS AND DISCUSSION

The aim of this work is to study the network structure and the related properties of ionic samples based on the commercial elastomer XNBR and different MgO contents and their evolution with the temperature, with a focus on molecular properties that are not accessible by other, previously used experimental techniques. A combination of different experimental techniques will be applied in this work in order to obtain a global picture including morphology, network structure, and dynamics in these complex and heterogeneous materials.

1. Phase Morphology. Metal oxides react with carboxylic groups grafted in the XNBR matrix forming the corresponding carboxylates salts.[23,57] This has been followed by FTIR-ATR (spectra not shown here) demonstrating that below the stoichiometric concentration (3.26 phr of MgO) both species (with vibration bands at 1698 cm^{-1} for carboxylic acid groups and 1591 cm^{-1} for the corresponding carboxylates, respectively) coexist, while at higher concentration only the carboxylates band is observed. These carboxylate moieties tend to aggregate into multiplets and clusters in a hierarchical structure that acts as cross-links forming a three-dimensional network (see Figure 1).

These ionic contacts drastically reduce the dynamics of polymer segments in the vicinity of ionic aggregates, creating layers of trapped polymer with gradually reduced mobility.[12,13] If aggregation is significant enough to create a phase-separated morphology, this polymer fraction shows its own thermal transition (named ionic transition[8]) as it is observed by dynamic mechanical thermal analysis (DMTA).[16] According to the variation of the loss factor with temperature (Figure 2), it is possible to relate the transition at lower temperatures with the T_g of the bulk polymer, whereas the ionic transition appears at higher temperatures only in elastomeric ionomers with phase-separated morphology.

At low MgO content (e.g., MgO-1) ionic transition appears at lower temperature, with an ionic transition temperature T_i, which is defined as the maximum of the broad ionic transition, around 50 °C. The addition of MgO up to the stoichiometric concentration shifts the transition to higher temperatures (around 80 °C). It seems to indicate the enhancement of the phase-separated morphology, i.e. the existence of two relatively well-defined dynamic environments corresponding to chain segments in bulk and those closer to the ionic aggregates, respectively. This could be explained by the thermodynamic tendency of carboxylic and carboxylate moieties to segregate and avoid the energetically unfavorable environment of the polymer chains.[8,15,58] In addition, the ionic transition becomes broader, indicating more complex and heterogeneous dynamics of the associated, trapped polymer segments. This behavior agrees with the dielectric relaxation measurements, which reveal differences of several decades in frequency between the two

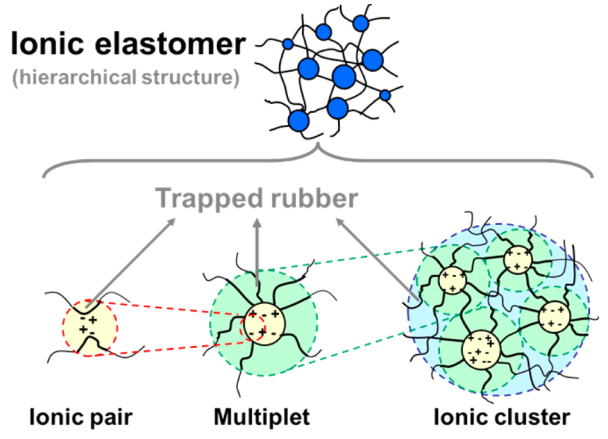

Figure 1. Schematic picture representing the hierarchical structure of ionic contacts that act as dynamic cross-link points in ionic elastomers.

dx.doi.org/10.1021/ma501208g | Macromolecules 2014, 47, 5655−5667

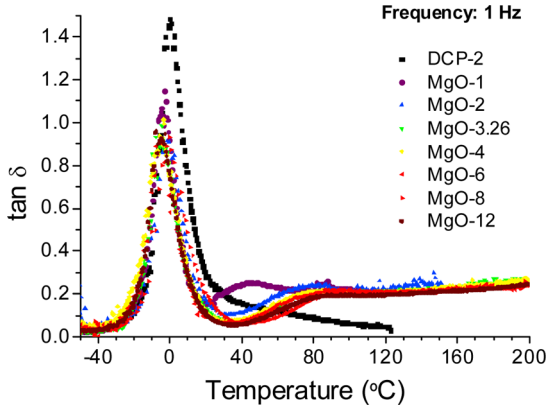

Figure 2. Variation of the loss factor (tan δ) with temperature at 1 Hz of ionic samples with different MgO content and a covalent sample cross-linked by dicumyl peroxide (DCP-2).

relaxing environments.[12,13] The addition of MgO above the stoichiometric concentration slightly shifts the ionic transition to higher temperatures.

2. Network Structure. *MQ NMR Measurements: Addressing the Coexistence of Weak and Strong Residual Dipole–Dipole Couplings.* In MQ NMR, two sets of data are recorded as a function of the DQ pulse sequence (evolution) time,[33,35,59] τ_{DQ}: the DQ build-up curve, I_{DQ}, and the reference decay curve, I_{ref}. The sum of both (after subtraction of a noncoupled defect contribution), $I_{\Sigma MQ} = I_{DQ} + I_{ref}$ − defects, is commonly used to obtain a point-by-point normalized build-up function, $I_{nDQ} = I_{DQ}/I_{\Sigma MQ}$, as it was explained elsewhere.[33,34,50] This latter function reflects the residual dipolar interactions related to the network structure (see the Supporting Information for more details).

In case of elastomeric ionomers (Figure 3a), the overall signal decay function in MQ experiments, $I_{\Sigma MQ}$, based upon the usual Baum–Pines (B–P) sequence exhibits a substantial overall loss of signal due to the limitation imposed by the minimum pulse sequence cycle time (~0.09 ms). This effect is rather weak for elastomers far above the glass transition temperature (T_g + 100 °C), but it poses a serious problem to characterize ionic elastomers because the trapped polymer with reduced dynamics is strongly dipolar-coupled (closer to the rigid limit ~30 kHz), and the associated signal decays almost completely during a single cycle of the B–P sequence.

To overcome this problem, a simplified version of the lengthy B–P sequence based upon the so-named five-pulse sequence was used.[60−62] In order to provide better stability and the long-time performance of the two-pulse segment for MQ excitation and reconversion, a refocusing π pulse was also introduced in each pulse sequence block, reaching a minimum pulse sequence cycle time of ~0.01 ms.

However, the improved five-pulse sequence is less efficient than the B–P approach at longer excitation times (required to characterize the weaker dipolar coupled segments between cross-links). This fact means that a combination of both experimental approaches is required to characterize both the *rigid* segments from the trapped polymer around ionic interactions and the *softer* rubber segments between cross-links.

To take into consideration the duty cycle dependent scaling factor, τ_{DQ} for the five-pulse sequence is scaled by a prefactor of 3/2 and thus render the data directly comparable.[33] In this way, the signals from both approaches superimpose at times close to the minimum B–P cycle time (see Figure 3a). The combined signal (Figure 3b) provides the complete information on this heterogeneous material composed by rubber segments in quite different dynamics regimes.

It is important to note the fast decay of the NMR signal caused by the strong dipolar coupled rubber segments. This causes the drop of $I_{\Sigma MQ}$ below 20% of its initial intensity at short τ_{DQ} times, increasing the uncertainties in the normalized I_{nDQ} build-up curve (see inset in Figure 3b). As consequence, the point-by-point normalization process, which is usually applied to separate both temperature-independent network structure effects and temperature-dependent segmental dynamics in elastomers,[33,34,50] does not seem to be the most appropriate methodology to extract dipolar coupling constants in elastomeric ionomers.

In order to prevent mathematical artifacts caused by the manipulation of weak signal intensities, $I_{\Sigma MQ}$ and I_{DQ} signals have been fitted simultaneously. It is important to remind that $I_{\Sigma MQ}$ only reflects information about the temperature-dependent segmental dynamics, while I_{DQ} depends on both temperature-independent network structure effects and segmental dynamics.[33] Since two rather well-separated dynamic processes

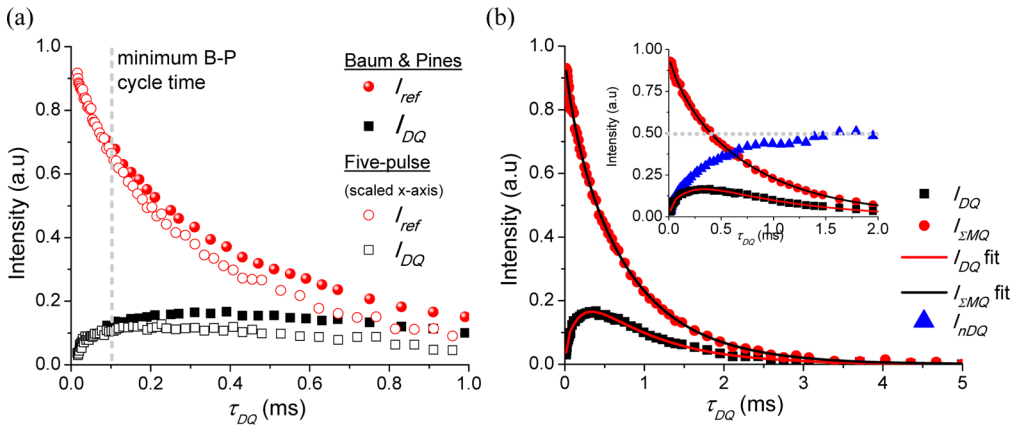

Figure 3. Proton MQ data for sample MgO-6 at 80 °C using (a) the B–P and five-pulse sequences. For the latter, the *x*-axis was scaled. The vertical dashed line identifies the minimum pulse sequence cycle time of B–P sequence. In (b) $I_{\Sigma MQ}$ and I_{DQ} signals were obtained by combining the intensities from both pulse sequences and fitted with eq 2 and eq 4, respectively. The inset shows the I_{nDQ} build-up curve obtained after normalization.

dx.doi.org/10.1021/ma501208g | *Macromolecules* 2014, 47, 5655−5667

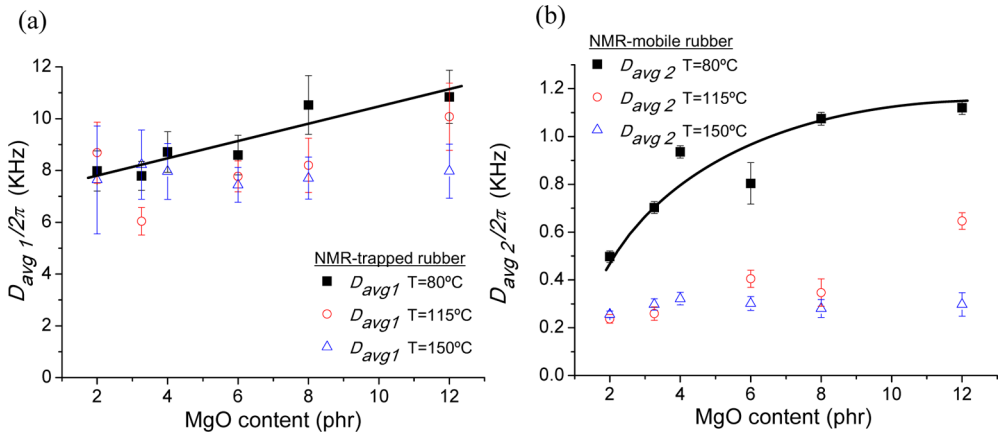

Figure 4. Dipolar coupling constant measured by MQ NMR (a) corresponding to the rigid rubber fraction (trapped polymer), D_{avg1}, and (b) corresponding to the mobile rubber fraction (rubbery polymer between constrains), D_{avg2}, as functions of the MgO content for ionic elastomers at temperatures of 80, 115, and 150 °C, respectively. Lines are only guides for the eyes.

coexist in the elastomeric ionomers, the $I_{\Sigma MQ}$ signal was fitted assuming two stretched exponential decay functions:

$$I_{\Sigma MQ} = B(A\,\exp(-2\tau_{DQ}/T_{2,1})^{\beta_1} + (1-A)\,\exp(-2\tau_{DQ}/T_{2,2})^{\beta_2}) \quad (2)$$

where B is the y-intercept value (e.g., fraction of dipolar coupled protons) and A is the trapped polymer fraction, whereas $T_{2,1}$ and $T_{2,2}$ are the characteristic relaxation times and β_1 and β_2 are the shape factors of the decay functions for the trapped rubber phase and the bulk (mobile) rubber, respectively.

Because of the chemical structure of the XNBR terpolymer and the complex and inhomogeneous network structure, the fits to the DQ build-up intensity, I_{nDQ}, which reflects the magnitude of the desired D_{res}, need to take into account a potentially broad distribution. Here, we could successfully use a build-up function defined by a gamma distribution of dipolar couplings (with a width defined by the average residual coupling D_{avg}),[53] see the Supporting Information for more details:

$$g(\tau_{DQ}, D_{avg}) = \int_0^\infty \frac{1}{2}\left(1 - \exp\left[-\frac{2}{5}{D_{res}}^2{\tau_{DQ}}^2\right]\right) \times \frac{2}{\sqrt{\pi}}\sqrt{\frac{27D_{res}}{8{D_{avg}}^3}}\,\exp\left(-\frac{3D_{res}}{2D_{avg}}\right)dD_{res} \quad (3)$$

The coexistence of weakly dipolar-coupled rubber segments between cross-links, and strongly dipolar-coupled segments that are trapped around ionic contacts, suggests the use of two gamma distributions in order to analyze both environments.

Taking into consideration both structural and dynamics requirements, I_{DQ} can be fitted by the expression

$$I_{DQ} = B(Ag_1(\tau_{DQ}, D_{avg1})\,\exp(-2\tau_{DQ}/T_{2,1})^{\beta_1} + (1-A)g_2(\tau_{DQ}, D_{avg2})\,\exp(-2\tau_{DQ}/T_{2,2})^{\beta_2}) \quad (4)$$

Upon simultaneous fitting of I_{DQ} and $I_{\Sigma MQ}$, the integrals are numerically evaluated within the environment of the Origin software, obtaining in all cases very good fittings as can be seen in Figure 3b. It is important to note that this analysis methodology provide comparable values respect to the most-used normalization process (see the Supporting Information).

Multiple-quantum (MQ) spectroscopy thus provides information about the accessible conformations of rubber segments (measured as $D_{avg,i}$) and segmental dynamics (relaxation times $T_{2,i}$) of rubber segments that form the trapped fraction (identified by A) and the bulk rubber. Nevertheless, only the structural information will be discussed in this section because the MSE-FID is a most reliable approach to quantify the actual trapped fraction, as it will be shown in the following sections.

Effect of MgO Content on Ionomer Network Structure. MQ NMR on the studied elastomeric ionomers at 80 °C reveals two distinguishable polymer behaviors (see Figure 4). On the one hand, the trapped rubber around the ionic aggregates is characterized by apparent dipolar coupling constants, D_{avg1}, around 9 kHz (Figure 4a), which is compatible with polymer segments with strong dipolar interactions closer to the rigid limit, and a time scale of segmental dynamics in the range of the inverse dipolar coupling strength. The situation is comparable to polymer segments measured not too far (a few tens of K) above the glass transition.[63−65]

On the other hand, D_{avg2} is in the range of 0.5−1 kHz (Figure 4b), and it is attributed to the order parameter of mobile rubber segments between constraints, i.e., the cross-link density. The correct assignment of D_{avg1} and D_{avg2} for ionomers was confirmed by using XNBR samples vulcanized with covalent cross-links, e.g. sample DCP-2, that show a single behavior characterized by dipolar coupling constants around 0.5 kHz (see Supporting Information).

Figure 4a shows a slightly increasing tendency (∼25%) of the dipolar coupling constant that characterizes the trapped polymer fraction with the MgO content. These results reflect a higher correlation between trapped rubber segments, which could be caused by the reduction on the available conformational space or the slowdown on their segmental dynamics. Nevertheless, the slight variation in the strength of ionic contacts with the addition of MgO has no measurable effect on the fraction of trapped polymer measured at 80 °C (see Figure 5). This important point will be discussed in the next sections by using the more efficient MSE-FID experiments to refocus the strong dipolar coupling interactions. It means that although both experimental approaches are able to characterize the fraction of trapped polymer, the latter is always somewhat more efficient in extracting quantitatively this information (see Supporting Information, Figure S6).

dx.doi.org/10.1021/ma501208g | *Macromolecules* 2014, 47, 5655−5667

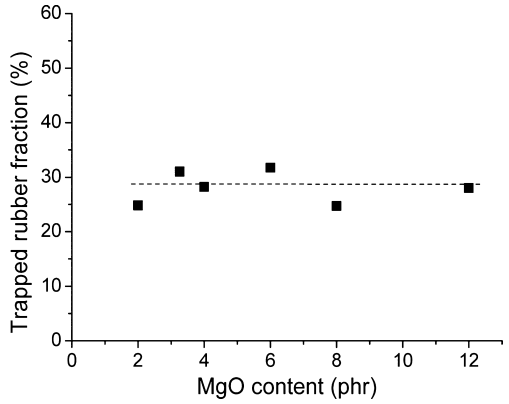

Figure 5. Evolution of trapped (rigid) rubber fraction around ionic contacts with the MgO content at 80 °C as measured by MQ NMR experiments. The dotted line is only a guide for the eyes.

Moreover, the addition of MgO leads to a clear increase of the cross-link density for XNBR ionomers as demonstrated in Figure 4b. Although the "rigid-limit" coupling D_{stat}/k, which takes into consideration a rescaling factor k that considers fast (~picoseconds) dynamics inside the statistical (Kuhn) segments, is not defined for the XNBR matrix, it was demonstrated that D_{avg2} is proportional to the cross-link density that characterize the rubber network.[33] The variation in the network structure with the concentration of MgO up to the stoichiometric concentration (3.26 phr) is explained by the increasing number of ionic moieties in the polymer backbone. Nevertheless, above that concentration, the number of carboxylates moieties remains constant, but the cross-link density continuously increases; therefore, the aggregation number, i.e. the number of ionic moieties per aggregate, has to be reduced. This interesting phenomenon is most likely related to the formation of additional interactions of ionic moieties with the excess of MgO, although the increase in the cluster (fixation) strength would be an additional factor to take into consideration.

Summarizing, the excess of MgO increases the cross-link density (higher value of D_{avg2}) and the fixation strength of polymer segments around ionic aggregates (higher dipolar strength, corresponding to the D_{avg1} value). These structural changes have measurable effects on the polymer dynamics and mechanical properties, as it will be demonstrated in the following sections.

Finally, MQ NMR was also applied to analyze the evolution of network structure with temperature (see Figure 4). In all cases, the dipolar coupling constant (in both trapped and mobile rubber phase) decreases, although the most important effect is observed in the behavior of the mobile rubber phase with the drop of D_{avg2} at temperatures above 80 °C (see Figure 4b). These results demonstrate that ionic aggregates loose their efficiency as cross-links (fixing points) on the time scale of the MQ NMR experiments (milliseconds range).

Ionic contacts are "dynamic bonds", which can selectively undergo reversible breaking and re-formation, usually under equilibrium conditions.[66] Both fast local rearrangements of ions inside the aggregates and slower collective rearrangements between aggregates have been identified previously.[67−69] The latter has been described via the ion-hopping mechanism between aggregates, although recent simulations point out the possibility that this process consists of cluster joining, rearranging (via ion exchanged through multiple local processes), and breaking.[67−69] Independently of the mechanism involved in the collective rearrangements between aggregates, this process provides the ionic aggregates with the ability to act as temporary cross-links similar to entanglements[70] with a characteristic lifetime τ, which becomes shorter with temperature. Therefore, the drop in D_{avg2} at elevated temperature qualitatively reveals the dynamic network structure of elastomeric ionomers, i.e., the loss of orientation correlation between chain segments due to the exploration of additional spatial conformations when collective rearrangements between clusters take place. The effect of this temperature-dependent process on polymer dynamics and mechanical properties will be discussed in more detail in the following sections.

3. Dynamic Heterogeneity and Phase Composition. *FID and MSE-FID Measurements and Analyses.* The simple free-induction decay (FID) signal in solid-state NMR is sensitive to the polymer mobility, and it can be used to study phase composition in polymers with well-separated dynamics by using the difference on dipolar coupling strength between the phases. Nevertheless, this simple procedure has one potential disadvantage in that, due to the relatively long dead time of low-field instruments, the initial part of the FID (related to the stronger dipolar coupled rubber segments) vanishes

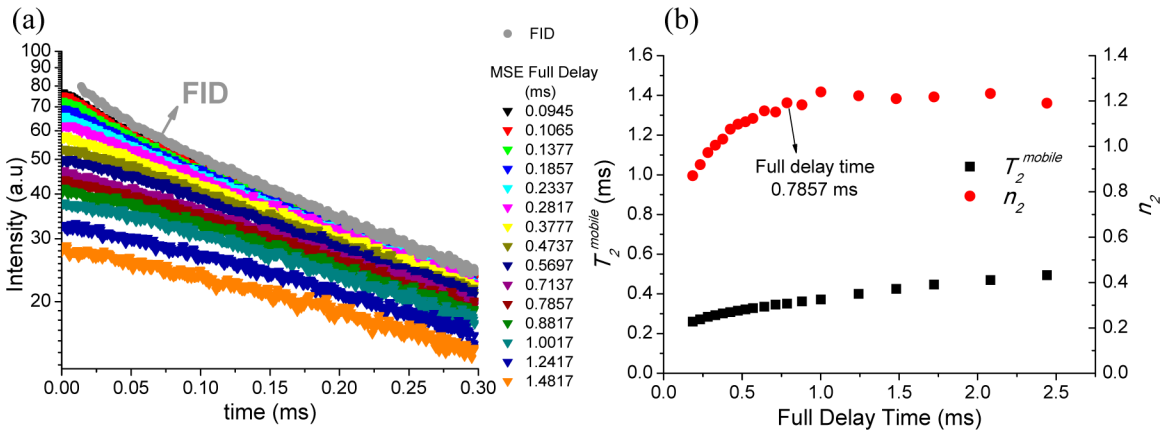

Figure 6. (a) FID and MSE-FID signals for MgO-6 sample measured at 80 °C by increasing the full delay time. The initial fast decay signal vanishes with the increment of the full delay time. (b) Variation of T_2^{mobile} and n_2 parameters with the full delay time. From times longer than 0.7857 ms the n_2 parameter achieves a plateau value. It indicates the minimum full delay time to relax the rigid signal.

dx.doi.org/10.1021/ma501208g | *Macromolecules* 2014, 47, 5655−5667

before the detection. Therefore, a magic sandwich echo (MSE) sequence was applied,[46,47] which is able to refocus the dipolar dephased signal and provide the shape of the entire signal decay (see Figure 6).

The signal obtained from elastomeric ionomers is a superposition of rigid trapped rubber around ionic moieties and highly mobile rubbery fraction between cross-links. Thus, a reliable analysis for the initial 0.3 ms of the refocused MSE-FID signals (Figure 6) was possible by using a weighted superposition of stretched exponential functions:[46,63,71]

$$I(t) = I_0[A \exp(-t/T_2^{\text{trapped}})^{n_1} + (1 - A) \exp(-t/T_2^{\text{mobile}})^{n_2}] \quad (5)$$

where I_0 is the initial intensity, A is the trapped polymer fraction, and T_2^{trapped} and T_2^{mobile} are the characteristic apparent relaxation times for trapped and mobile phase, respectively, whereas n_1 and n_2 are shape exponents (stretching or compressing the exponential function) for both phases.

According to the MSE pulse sequence detailed in previous papers,[46,47] it is further possible to lengthen the interpulse delays in order to identify and characterize the relaxation behavior of the individual components that coexist in these heterogeneous samples (Figure 6a). In this case, different phase switching times, τ_φ, were used to change the total sequence length. Hence, the initial fast decaying signal, which is attributed to trapped rubber, vanishes first by increasing the full delay time (Figure 6a). According to the fitting results shown in Figure 6b, the full delay time of 0.7857 ms is large enough to filter out the immobilized-domain signal and obtain a single stretched exponential (with constant n_2 values) that characterizes the decay behavior for mobile rubber phase in the elastomeric ionomers.

The parameters T_2^{mobile} and n_2 obtained by the analysis of MSE-FID signal at full delay time of 0.786 ms were fixed, whereas the parameters that define the rigid rubber fraction (A, T_2^{trapped}, and n_1) varied freely in the fitting procedure of MSE-FID signal with the shortest full delay time of 0.095 ms according to eq 5. At this point it is important to take into account the loss of efficiency in the MSE sequence when molecular motions reach a characteristic time scale (0.1−0.01 ms) of the same order of the inverse refocused interaction ($D_{\text{avg1}} \sim 10$ kHz from MQ experiments).[63,70] In the case of elastomeric ionomers with phase-separated morphology, we expect a broad distribution of correlation times caused by the trapped rubber around ionic moieties. It means that rubber segments in this intermediate motional regime (mostly the trapped rubber) may be underestimated by using MSE sequence. For this reason, unrefocused FIDs always show higher intensities than MSE-FID signals (see Figure 6a as an example), and they were used to quantify the trapped rubber fraction. To achieve this, the shape parameters of individual components, which were independently obtained by using MSE-FID signals at different switching times, were fixed in eq 5 to fit the FID signal and quantitatively obtain the trapped rubber fraction. This analysis strategy was successfully used to characterize the glassy rubber fraction around filler particles in reinforced rubbers.[63,64,71]

Trapped Rubber Fraction. Effect of MgO Content. In the investigated range of MgO contents and temperatures, the fitted apparent T_2 relaxation times varied between $T_2^{\text{trapped}} \sim 0.05-0.10$ ms and $T_2^{\text{mobile}} \sim 0.40-0.80$ ms for the trapped and mobile rubber fractions, respectively. The trends of their variation (data not shown) roughly follow the trends discussed above for the respective (inverse) residual dipolar coupling values, demonstrating that the T_2 relaxation behavior is dominated by (motionally averaged) dipolar interactions. They are additionally influenced by the actual segmental dynamics time scale as well as the shim limit (B_0 field inhomogeneity) in the case of T_2^{mobile} when it reaches the milliseconds range. We therefore refrain from a more detailed discussion and just repeat the salient conclusion from the MQ NMR experiments, which indicated a reduced aggregation tendency of ionic moieties, higher cross-link density, and stronger fixation strength of polymer segments around ionic aggregates with the MgO content.

Unaffected by these structural changes, the fraction of rubber with restricted mobility remains constant above the MgO stoichiometric concentration, as it is shown now quantitatively in Figure 7.

Below the stoichiometric limit, carboxylic groups are just partially neutralized by the with the metal oxide; for that reason a weak increase of trapped rubber faction is evidenced in Figure 7 up to complete neutralization is reached. At this point, a constant trapped rubber faction is always observed. These results demonstrate that each ion pair (independently of the aggregate structure) effectively anchors the polymer segments in the proximity of the ionic moiety, reducing their mobility.

It is important to stress the differences in the trapped rubber fraction obtained by the application of different experimental techniques, as the results may differ widely owing to the underlying sensitivity of the respective techniques. The NMR approach unambiguously reveals that up to 60% of polymer segments are firmly anchored to the ionic aggregates and show restricted mobility at 40 °C. This is 3 times larger than the value obtained by analyzing the area under the curve in DMTA, which indicates the presence of 15−20% of trapped rubber (data not shown). In the latter experiments, the rubber fraction with restricted mobility has to be large enough (usually ionic clusters) to show phase separated behavior with a characteristic thermal transition. This means that DMTA is insensitive to rubber segments with restricted mobility around ionic pairs and/or insolated multiplets, whereas time-domain NMR experiments provide more local and quantitative analysis based upon actual mobility information.

In a similar sense, the thickness of the restricted-mobility layer obtained by the popular analysis of X-ray diffraction profiles (usually by using the Yarusso−Cooper model[17]) is also subject to some limitations. Quantitative analysis has to assume

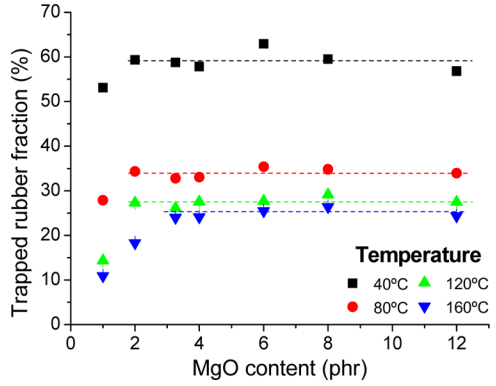

Figure 7. Evolution of trapped (rigid) rubber fraction around ionic interactions with the MgO content at different temperatures. Dotted lines are only guides for the eyes.

dx.doi.org/10.1021/ma501208g | *Macromolecules* 2014, 47, 5655−5667

that all trapped polymer is phase-separated, and it scatters because of a different electron density. Nevertheless, it was proven (see the Supporting Information for more details) that this technique is not sensitive to small scattering entities randomly dispersed in the matrix (which is in fact the main structural effect of adding increasing amounts of MgO according to the NMR results) because their increasing presence changes the matrix scattering. The problems to quantify the actual trapped rubber fraction seem to be overcome by using the NMR approach.

Effect of Temperature. The main advantage of ionic elastomers over conventional (covalently cross-linked) elastomers is their thermoplastic behavior. At high temperature, ionic elastomers can be melt-processed under low-shear conditions, e.g. compression molding, and losing their elastic properties upon processing due to the increased mobility of ionic pairs and their ability to rearrange between aggregates. For that reason, it is mandatory to characterize the effect of temperature on rubber mobility.

Figure 7 shows the decreasing fraction of trapped polymer when samples are heated because different rubber layers around the ionic clusters become mobilized at different temperatures. Nevertheless, it is important to point out that above the MgO stoichiometric concentration (3.26 phr) a rather high fraction of immobilized polymer segments (∼30%) is detectable by NMR up to 160 °C. This result has two main consequences: (i) ionic pairs remain active as (dynamic) anchoring points on the sub-ms time scale (at high temperatures), and (ii) the fraction of trapped polymer segments in the high-temperature regime is at least of the order of magnitude of the volume spanned by a polymer persistence length around an idealized ionic contact.

Complementarily, we have already seen a molecular proof that the residual dipolar coupling of the matrix drops substantially at elevated temperature (Figure 4b), reflecting the loss of efficiency of ionic interactions as elastically active cross-links in the milliseconds time scale. These complementary results are quite important because ionic contacts can be understood as dynamic bonds,[66−69] which can selectively undergo reversible rearranges between aggregates after a certain characteristic lifetime. Consequently, their efficiency as active cross-link points strongly depends on the studied time scale.

In order to address the effect of ionic rearrangement lifetimes on the terminal chain dynamics, we studied this process by applying the frequency−temperature superposition principle[49] to the data obtained from the rubber process analyzer, in order to obtain a master curve that represents the stress relaxation of the shear modulus (G') in a wide range of frequencies for different XNBR samples (see Figure 8). Polymer chains in XNBR ionomers can flow via ionic exchanged between discrete aggregates without breaking all their ionic associations simultaneously, but this slow process requires high temperatures to take place on manageable time and frequency scales. Opposite to this behavior, the XNBR matrix covalently cross-linked by using 2 phr of dicumyl peroxide (sample DCP-2 in Figure 8) reveals a clear elastic plateau over a wide range of temperatures and frequencies.

In the XNBR ionomers, there are noticeable differences in the flow properties as a function of MgO concentration. The slower chain dynamics of elastomeric ionomers with higher amount of MgO could be related with the higher number of ionic aggregates (along the same lines as inferred from the NMR results). This means that any polymer segment requires larger number of ionic rearrangements between nearest-neighbor aggregates to explore the same space for XNBR ionomers with higher cross-link density.

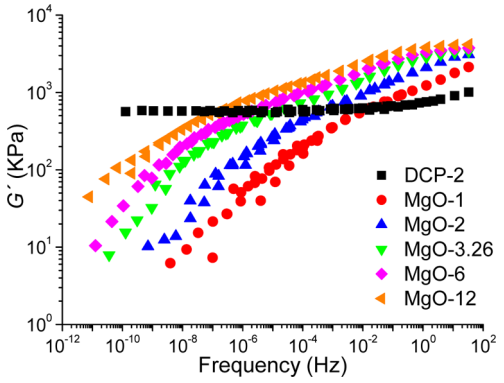

Figure 8. Flow curves of ionic samples and a covalent sample obtained by measuring the shear modulus at different frequencies and temperatures, plotted for a reference temperature of 40 °C. The displacement factors used for frequency−temperature superposition were different for each sample.

4. Network Structure−Property Relationships. *Properties at Room Temperature.* The complex network structure and chain dynamics of elastomeric ionomers determines the physical properties of these materials and their evolution with temperature. As it is demonstrated in Table 1, elastomeric ionomers based on XNBR matrix show excellent and improved properties at room temperature as compared to the covalent network counterpart (DCP-2). Ionic multiplets, which are formed by the association of ionic groups and immobilized rubber (60% of trapped polymer according to NMR measurements at 40 °C), behave as reinforcing sites increasing the hardness, the stress at constant strain (usually named modulus in the rubber field), the tensile, and tear strength and reducing the abrasion loss of ionic elastomers with respect the covalent networks.[48]

Nevertheless, in opposition to the adverse effect of conventional reinforcing fillers (e.g., silica or carbon black particles) on the ultimate properties of the rubber,[72,73] the existence of an ion-rich phase in ionomers enhances the elongation at break of XNBR networks due to the dynamic nature of cross-links based on the collective ionic rearrangements during deformation. For this reason, overstrained chain segments have the ability to pull out the ionic moieties from their original multiplets (cross-link points) and subsequently reform in another ionic aggregate. This dynamic process promotes the stress relaxation and prevents the premature failure of the matrix, allowing for elongations at break above 600% (twice that of a covalent network). Obviously, this dynamic process is a dissipative mechanism that has a negative effect on the compression set values showed by these materials at room temperature.

Differences in the ionic network structure arising from changes in the MgO content are correlated with the variation of mechanical properties of these ionomers. The formation of a higher number ionic interactions with lower aggregation number increases the overall number of effective cross-links (reflected in D_{avg2}) and the stiffness of the trapped rubber region (reflected in D_{avg1}). However, the fraction of trapped rubber is constant at MgO concentrations above the stoichiometric concentration. These structural modifications cause the enhancement of modulus at a given deformation of the tensile strength and the hardness in ionomers.

dx.doi.org/10.1021/ma501208g | *Macromolecules* 2014, 47, 5655−5667

Table 1. Physical Properties Measured at Room Temperature for the Studied XNBR Samples

samples	M100[a] (MPa)	M300[a] (MPa)	M500[a] (MPa)	TS[b] (MPa)	EB[c] (%)	tear S[d] (kN/m)	AL[e] (mm^3)	hardness shore A	CS$^{(1)f}$ T_{room} (%)	CS$^{(2)f}$ T = 70 (%)
DCP-2	1.13 ± 0.01	2.7 ± 0.1		2.8 ± 0.3	302 ± 9	9.5 ± 0.9	279 ± 63	43.1 ± 0.4	5.1 ± 0.2	6.5 ± 0.2
MgO-2	3.39 ± 0.06	6.7 ± 0.2	16 ± 2	37 ± 7	615 ± 43	43.6 ± 0.7	64 ± 2	61.9 ± 0.9	52 ± 1	86 ± 5
MgO-3.26	4.25 ± 0.08	9 ± 0.3	22 ± 1	45 ± 4	616 ± 14	50 ± 4	77 ± 3	69 ± 1	48 ± 2	95 ± 3
MgO-4	5.0 ± 0.1	10.6 ± 0.2	24.6 ± 0.9	50.1 ± 0.9	627 ± 174	55 ± 4	78 ± 3	72 ± 1	47 ± 2	89.4 ± 0.2
MgO-6	5.7 ± 0.2	12.2 ± 0.3	28 ± 1	52.3 ± 0.9	623 ± 9	59 ± 5	83 ± 2	74.6 ± 0.5	47 ± 1	92 ± 1
MgO-8	6.3 ± 0.1	13.4 ± 0.1	29.1 ± 0.7	51 ± 2	637 ± 43	53 ± 6	86 ± 1	75.9 ± 0.6	44 ± 1	85.8 ± 0.1
MgO-12	7.2 ± 0.2	15.3 ± 0.4	32 ± 3	53 ± 2	619 ± 12	61 ± 0.8	87 ± 1	77 ± 0.3	43 ± 4	83 ± 2

[a]Modulus at 100%, 300%, and 500% deformations, respectively. [b]Tensile strength. [c]Elongation at break. [d]Tear strength. [e]Abrasion loss. [f]Compression Set at room temperature (1) and 70 °C (2), respectively.

These results and the observed linear correlation between the stress at a constant strain and the dipolar coupling constant measured by MQ NMR experiments (Figure 9) demonstrate that the cross-link density, i.e., the number of ionic aggregates, is the main factor that determines the properties of fully neutralized elastomeric ionomers. In addition, linear fits are compatible with lines that go through the origin; i.e., the actual entropic rubber elasticity dominates the mechanical properties of ionic elastomers (thus being similar to unfilled covalently cross-linked rubbers[1]) with a minimal influence of additional factors. In this sense, the excess of MgO particles above the stoichiometric concentration corresponds to a very minor volume fraction that is hardly relevant in the physical properties of these compounds (taking as reference the behavior of traditional reinforcing filler particles, e.g., silica and carbon black, used in rubber technology[73]).

Although the ionic samples contain high fraction of trapped polymer in ion-rich aggregates that act as filler particles, there is no visible additional effect of their potential aggregation (filler networking similar to filled rubber samples with high content of silica and/or carbon black) as it was proven by the strain-sweep experiments reported in Figure 10.

A sigmoidal drop in the storage modulus G' in strain sweep experiments (the so-called Payne effect[74]) is widely reported in rubber composites when a percolation network of solid particles is formed;[73−76] however, XNBR samples do not show this behavior with almost constant G' value along the studied strain range.

These evidences indicate the absence of an independent mechanical contribution from a potential network formed by immobilized polymer layers around ionic aggregates; rather, the ionic clusters act as isolated, only hydrodynamically active filler particles. The hydrodynamic effect caused by the presence of nondeformable (or at least much less deformable) trapped polymer regions inside a softer matrix should be taken into account to understand the enhanced mechanical properties of elastomeric ionomers with respect their covalently cross-linked counterparts. In this sense the fraction of trapped polymer that act as filler was roughly estimated by using the Guth−Gold ($G'/G'_0 = 1 + (5/2)\phi + 14.1\phi^2$) and Padé ($G'/G'_0 \approx 1 + (5/2)\phi + 5.0\phi^2 + ...$) approaches[77] for samples measured at 40 °C (Figure 10). In this case the immobilized polymer fractions ϕ were determined by comparing the storage modulus G' for the "reinforced" ionic system (MgO-4) and G'_0 coming from an "unfilled" covalent counterpart (DCP-4), where the latter was the highest covalent cross-linked sample that withstood large strains. We thus need to consider that the covalently cross-linked sample has a cross-link density that is only a half of the ionic network, introducing a factor of 2 for the estimations of ϕ. As it is shown in Figure 10, both approaches indicate that the increase in the storage modulus of the ionic elastomers can be explained by a hydrodynamic effect of around 15−20% of rigid polymer inside the XNBR matrix. This rough estimate deviates from the NMR results that are sensitive to all the immobilized rubber segments (Figure 7), which is of course due to the fact that the immobilized rubber represents a "soft" filler.[78] Using eq 8.30 in ref 78, $(G'/G'_0 = 1 + (5/2)\phi\{(G'_f/G'_0 - 1)/[G'_f/G'_0 +$

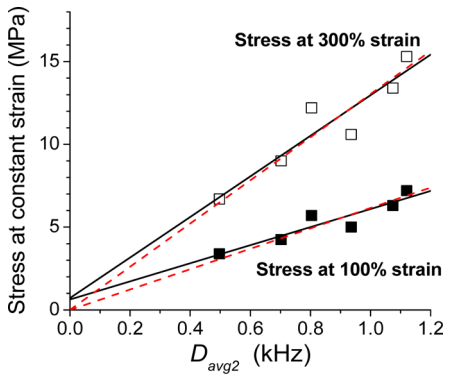

Figure 9. Correlation of stress at constant strain (100% and 300%, respectively) at room temperature with the dipolar coupling constant at 80 °C, i.e., the cross-link density, as measured by NMR for ionic elastomers. Solid lines show the linear fit for the experimental data whereas dashed lines are the linear fits forced to go through the origin.

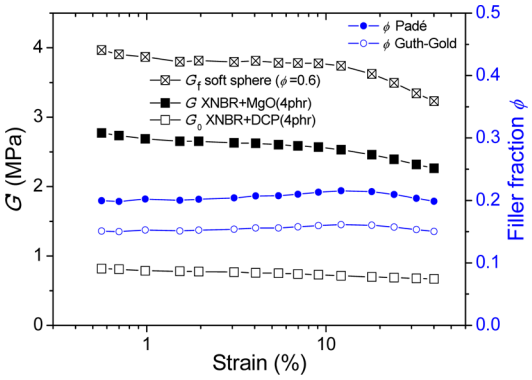

Figure 10. Storage modulus G' and rigid polymer fraction versus shear strain amplitude to evaluate a possible Payne effect for ionic (MgO-4) and covalent (DCP-4) samples at 40 °C. The apparent rigid polymer fraction plotted was estimated via the Guth−Gold or Padé approaches, considering that the modulus of the rubber matrix estimated by NMR in the MgO sample ($D_{avg2}/2\pi \sim 1$ kHz, Figure 4) is about twice that of the DCP sample ($D_{avg2}/2\pi \sim 0.5$ kHz, Figure S3). A soft-sphere approach can be used to estimate the apparent modulus of the filler G'_f.

dx.doi.org/10.1021/ma501208g | Macromolecules 2014, 47, 5655−5667

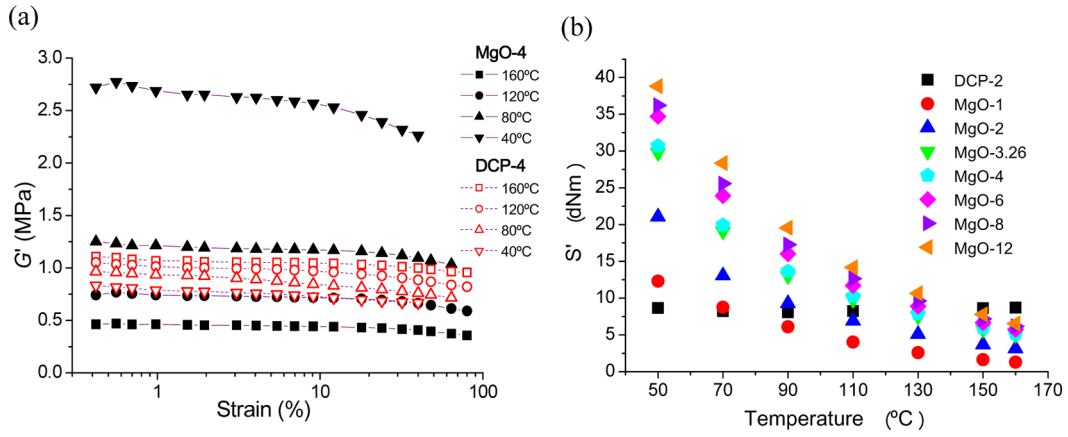

Figure 11. (a) Storage modulus G' in function of the shear strain amplitude (Payne effect) measured at different temperatures for an ionic (MgO-4) and a covalent (DCP-4) sample, respectively. (b) Variation of the elastic component of torque S' obtained from the RPA at 6.98% deformation, 1.667 Hz, and variable temperatures.

$3/2 - \phi(G'_f/G'_0 - 1)]\}$, that describes the reinforcement effect of soft-sphere fillers with finite modulus G'_f, we can use the NMR result for $\phi \approx 0.6$ to estimate a reasonable value for G'_f as plotted in Figure 10.

Properties at Elevated Temperature. MgO-cross-linked ionomers and permanently DCP-cross-linked counterparts are strictly comparable only at low temperatures. To illustrate this fact, the variation of elastic properties with temperature for XNBR samples is shown in Figure 11.

The storage modulus increases with temperature in the covalently cross-linked networks (e.g., DCP-4 sample in Figure 11a) according to their thermostable behavior and the entropic origin of rubber elasticity.[1] At room temperature, ionic samples (e.g., MgO-4) reach storage moduli that are about 3.5 times larger than those obtained for the covalent network because of the existence of high fraction of trapped rubber as well as their higher effective cross-link densities as estimated by NMR experiments. However, the rise of temperature leads to faster dynamics of the ionic pairs (ionic rearrangements of aggregated ions) and an enhanced mobility for the polymer close to the ionic aggregates. As a result, G' continuously decreases for ionic samples with temperature, until it falls below the value of the covalent network (Figure 11a). It is important to remind that ionic aggregates do not disappear with temperature as it was demonstrated in NMR measurements by the persistence of trapped rubber with restricted dynamics but they lose their efficiency as cross-links on the milliseconds time scale because of their dynamic nature.

It is also important to mention that the storage modulus remains almost constant with the strain amplitude for XNBR samples, independently of temperature. This validates the evaluation of the elastic component of torque (S') of ionic samples obtained from the rubber process analyzer (RPA) at different temperatures in Figure 11b, for which a strain beyond the usual linear range was used.

These data demonstrate that formation of more ionic anchor points with lower aggregation number by the addition of increasing amounts of MgO enhances the elastic properties measured at elevated temperature because of the slower terminal dynamics (Figure 8). Nevertheless, the differences in S' become weaker at high temperature (160 °C) as compared to the large variations of torque at lower temperature (50 °C). Obviously, these results depend on the time frame of the experiments, since it was demonstrated (Table 1) that differences between ionic elastomers completely disappear in experiments with larger time windows, e.g., compression set experiments performed at 70 °C. In those experiments, ionic groups are able to diffuse between ionic interactions and completely reorganize the network structure. This dissipating mechanism promotes the stress relaxation of polymer chains and on consequence, only ~10% (in average) of energy is stored by these samples.

CONCLUSIONS

Elastomeric ionomers have unique physical and processing properties compared to their covalently cross-linked counterparts due to their hierarchical structure and dynamic nature of ionic interactions, the ionomer phase morphology, network structure, and chain dynamics. However, the characterization of elastomeric ionomers was demonstrated to be a complex challenge due to the multiple time and length scales involved, requiring the use of complementary experimental approaches to obtain a complete picture of these structurally and dynamically heterogeneous materials. In this work, the combination of different advanced time-domain NMR strategies, i.e., MQ spectroscopy and component analysis of MSE-FIDs, performed in low-field spectrometers has been shown as a useful, versatile, and powerful tool to obtain local information that gives new insights into the network structure and rubber mobility in elastomeric ionomers.

The addition of MgO promotes the conversion of carboxylic moieties, which are directly grafted to the XNBR polymer backbone, to the corresponding carboxylate salts. Upon increasing the degree of neutralization, it was demonstrated that the distance between the ionic moieties decreases, enhancing their aggregation trend. The strength of ionic contacts rises, as well as the firmness with which polymer segments are anchored by the corresponding ionic pairs. Therefore, the fraction of trapped rubber with restricted mobility shows an appreciable increase, and the phase-separated morphology is enhanced.

Above the stoichiometric concentration, the neutralization process is completed, but the addition of increasing amounts of MgO limits the aggregation state of the existing ionic groups, thus altering the network structure and the physical properties of XNBR ionomers. An excess of MgO promotes the formation of a higher number of ionic aggregates with lower aggregation number (i.e., the number of ionic pairs per multiplet and/or

dx.doi.org/10.1021/ma501208g | Macromolecules 2014, 47, 5655−5667

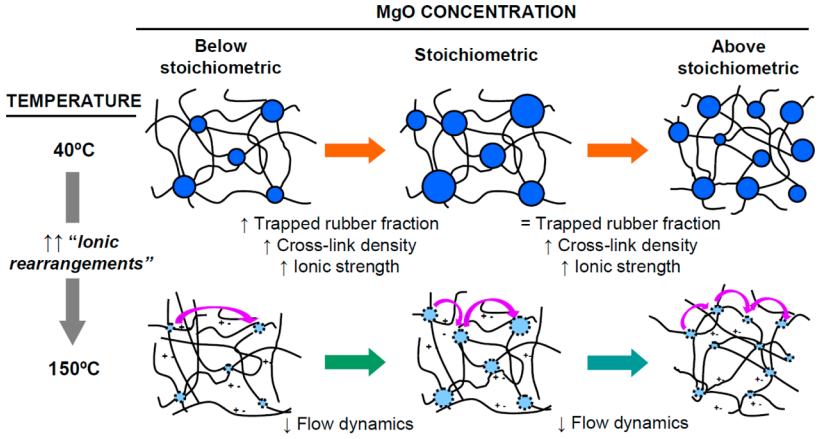

Figure 12. Schematic picture summarizing the effect of MgO concentration and temperature on the ionomer network structure and ion hopping dynamics, respectively.

cluster is reduced), as indicated by the overall increase in the cross-linking density as measured by MQ-NMR. These variations in the structure of ionic aggregates impose stronger constraints on the local mobility of the polymer segments in the proximity of the anchoring points but have no appreciable effect on the fraction of trapped polymer, which remains constant as it was measured by means of MSE-FID experiments.

The structural changes in XNBR ionomers caused by the addition of MgO are schematically shown in Figure 12.

According to the dynamic nature of ionic moieties, it is mandatory to understand the temperature dependence of structural and dynamics parameters that govern the behavior of these elastomeric ionomers. The results from NMR and rheological experiments confirm that temperature enhances the mobility of polymer chains and speeds up the collective ion rearrangement between aggregates.

The fraction of immobilized rubber around ionic interactions (approximately 60% of polymer at room temperature) continuously decreases with temperature, suggesting the existence of a motional gradient with a distribution of polymer dynamics. However, a significant fraction of immobilized polymer segments (~30%) remains detectable by NMR at high temperature (up to 160 °C). These results demonstrate that at very short time scales most of the ionic pairs remain active as anchoring points, and consequently, polymer segments in the proximity of ionic moieties show reduced mobility on a length scale of the persistence length of the rubber chain, independently of the aggregate morphology. These statements identify the concentration of ionic moieties grafted to the rubber backbone and the polymer persistence length as the most important factors that determine the immobilized polymer fraction, whereas the state of aggregation, i.e., the hierarchical structure of ionic interactions, plays a minor role.

On a different (larger) time scale it is possible to observe how the slow cooperative movements, related to the cooperative ion rearrangement mechanism, are stimulated with temperature. In this sense, ionic interactions could be defined as temporal and dynamic anchor points where ionic moieties reside for a certain time until the next exchange. These dispersive phenomena dominate the ionomer behavior when the time scale associated with the studied process is longer than the characteristic residence time. However, at shorter times, ionic interactions behave as "fixed" anchor points, and ionomers give an elastic response. This fact enables the combination of excellent elastic properties at room temperature and processing advantages at high temperature. We noticed huge differences in the frequency (around 3 orders of magnitude according rheological measurements) of the polymer flow dynamics for XNBR ionomers vulcanized with different concentrations of MgO. These results seem to confirm the formation of higher number of ionic interactions that slow down the terminal dynamics since ionic groups require larger number of rearrangements to flow. The effect of temperature on trapped rubber and ion rearrangement dynamics is schematically represented in Figure 12.

The complex network structure and chain dynamics of elastomeric ionomers described previously determines the physical properties of these materials and their evolution with temperature. The significant fraction of immobilized polymer around discrete ionic clusters enhances the stiffness of ionic networks respect to the covalent counterparts without any evidence of a drop in mechanical properties at high strain amplitudes. In addition, the ability of ionic moieties to exchange between multiplets (induced by the strain at room temperature) redistributes the stress in a healing process and consequently enlarges the elongation at break of ionomers. This statement is also valid to understand the physical properties of ionomers with different neutralization degree.

We finally stress again our central result, which is that the enhancement of modulus at a given deformation, tensile strength, and hardness with excess of MgO is mainly caused by the variation in the ionic network structure, e.g., formation of higher number of ionic interactions with lower aggregation number that increases the overall number of cross-links, keeping the fraction of trapped (rigid) rubber constant. This fact stresses the importance of cross-link density (rubber elasticity) to understand the elastic properties of fully neutralized elastomeric ionomers, as it was demonstrated by the complete absence of additional filler networking effects from the immobilized polymer entities associated with ionic moieties.

This work clearly identifies unique qualitative relationships between the network structure and rubber mobility with the exceptional elastic properties of elastomeric ionomers. More in-depth low-field solid-state NMR investigations and data analyses strategies are necessary to obtain information on the

dx.doi.org/10.1021/ma501208g | *Macromolecules* 2014, 47, 5655−5667

exact time scales of segmental and chain motion, thus possibly more quantitatively matching results from other (more commonly used) complementary techniques. However, the pronounced structural and dynamic inhomogeneity of elastomeric ionomers remains an important challenge for any technique.

■ ASSOCIATED CONTENT

Supporting Information

MQ NMR analysis procedure and experimental details; Figures S1−S12. This material is available free of charge via the Internet at http://pubs.acs.org.

■ AUTHOR INFORMATION

Corresponding Authors

*E-mail malonso@ictp.csic.es (M.A.M.).
*E-mail kay.saalwaechter@physik.uni-halle.de (K.S.).
*E-mail jlvalentin@ictp.csic.es (J.L.V.).

Notes

The authors declare no competing financial interest.

■ ACKNOWLEDGMENTS

The authors thank CICYT for the financial support of this work (MAT 2008/02362 and MAT 2011-23476, MAT2011/23455 and MAT2011/-12921-E). M.A.M. and A.G.J. also express their gratitude to Consejo Superior de Investigaciones Científicas (CSIC) for their fellowships, Jae-Pre-088 and Jae-Pre-CP, respectively. J.L.V. thanks Ministerio de Ciencia e Innovación (Spain) for his Ramon y Cajal contract.

■ REFERENCES

(1) Treloar, L. R. G. *The Physics of Rubber Elasticity*; Oxford University Press: London, 1958.
(2) Brydson, J. A. *Rubber Chemistry*; Applied Science Publishers LTD: London, 1978.
(3) Alliger, G. S.; Sjothun, I. J. *Vulcanization of Elastomers*; Reinhold Publishing Corporation: New York, 1964.
(4) Eirich, F. R. *Science and Technology of Rubber*; Academic Press, Inc.: New York, 1978.
(5) Legge, N. R.; Holden, G.; Schroeder, H. E. *Thermoplastic Elastomers. A Comprehensive Review*; Carl Hanser Verlag: Munich, Germany, 1987.
(6) Holden, G.; Kricheldorf, H. R.; Quirk, R. P. *Thermoplastic Elastomers*; Carl Hanser Verlag: Munich, Germany, 2004.
(7) Eisenberg, A. K.; Kim, J. S. *Introduction to Ionomers*; John Wiley & Sons, Inc.: New York, 1998.
(8) Eisenberg, A.; Hird, B.; Moore, R. B. *Macromolecules* **1990**, *23*, 4098−4107.
(9) Kurian, T.; Khastgir, D.; De, P. P.; Tripathy, D. K.; De, S. K.; Peiffer, D. G. *Polym. Int.* **1996**, *37* (3), 413−419.
(10) Wouters, M. E. L.; Goosens, J. G. P.; Binsbergen, F. L. *Macromolecules* **2002**, *35*, 208−216.
(11) Rodríguez, A.; Ibarra, L.; Mora, I. *J. Appl. Polym. Sci.* **2007**, *106*, 973−980.
(12) Castagna, A. M.; Wang, W.; Winey, K. I.; Runt, J. *Macromolecules* **2011**, *44* (13), 5420−5426.
(13) Castagna, A. M.; Wang, W.; Winey, K. I.; Runt, J. *Macromolecules* **2011**, *44* (8), 2791−2798.
(14) Macknight, W. J.; Earnest, J. R. *J. Polym. Sci., Part D: Macromol. Rev.* **1981**, *16*, 41−122.
(15) Eisenberg, A. *Macromolecules* **1970**, *3* (2), 147−154.
(16) Hird, B.; Eisenberg, A. *Macromolecules* **1992**, *25*, 6466−6474.
(17) Yarusso, D. J.; Cooper, S. L. *Macromolecules* **1983**, *16*, 1871−1880.
(18) Wouters, M. E. L.; Litvinov, V. M.; Binsbergen, F. L.; Goosens, J. G. P.; Van Duin, M.; Dickland, H. G. *Macromolecules* **2003**, *36*, 1147−1156.
(19) Van der Mee, M. A. J.; ĹAbbe, R. M. A.; Portale, G.; Goosens, J. G. P.; Van Duin, M. *Macromolecules* **2008**, *41*, 5493−5501.
(20) Sun, C. X.; Van der Mee, M. A. J.; Goosens, J. G. P.; Van Duin, M. *Macromolecules* **2006**, *39*, 3441−3449.
(21) Litvinov, V. M.; Braam, A. W. M.; Van Der Ploeg, A. F. M. J. *Macromolecules* **2001**, *34*, 489−502.
(22) Ibarra, L.; Alzorriz, M. *Polym. Int.* **2000**, *49* (1), 115−121.
(23) Ibarra, L.; Alzorriz, M. *J. Appl. Polym. Sci.* **2002**, *87*, 805−813.
(24) Ibarra, L.; Alzorriz, M. *J. Appl. Polym. Sci.* **2007**, *103* (3), 1894−1899.
(25) Marx, C. L.; Caulfield, D. F.; Cooper, S. L. *Macromolecules* **1973**, *6* (3), 344−353.
(26) Dalmas, F.; Leroy, E. *Macromolecules* **2011**, *44* (20), 8093−8099.
(27) Laurer, J. H.; Winey, K. I. *Macromolecules* **1998**, *31* (25), 9106−9108.
(28) Moffitt, M.; Eisenberg, A. *Macromolecules* **1997**, *30* (15), 4363−4373.
(29) Basu, D.; Das, A.; Stöckelhuber, K. W.; Jehnichen, D.; Formanek, P.; Sarlin, E.; Vuorinen, J.; Heinrich, G. *Macromolecules* **2014**, *47* (10), 3436−3450.
(30) Mani, S.; Weiss, R. A.; Williams, C. E.; Hahn, S. F. *Macromolecules* **1999**, *32* (11), 3663−3670.
(31) Weiss, R. A.; Yu, W. C. *Macromolecules* **2007**, *40* (10), 3640−3643.
(32) Litvinov, V. M.; De, P. P. *Spectroscopy of Rubbers and Rubbery Materials*; Rapra Technology Ltd.: Shawbury, UK, 2002.
(33) Saalwächter, K. *Prog. Nucl. Magn. Reson. Spectrosc.* **2007**, *51* (1), 1−35.
(34) Valentín, J. L.; Posadas, P.; Fernández-Torres, A.; Malmierca, M. A.; González, L.; Chassé, W.; Saalwächter, K. *Macromolecules* **2010**, *43* (9), 4210−4222.
(35) Saalwächter, K.; Ziegler, P.; Spyckerelle, O.; Haidar, B.; Vidal, A.; Sommer, J. U. *J. Chem. Phys.* **2003**, *119*, 3468−3482.
(36) Saalwächter, K.; Herrero, B.; López-Manchado, M. A. *Macromolecules* **2005**, *38* (23), 9650−9660.
(37) Vaca Chávez, F.; Saalwächter, K. *Macromolecules* **2011**, *44* (6), 1549−1559.
(38) Callaghan, P. T.; Samulski, E. T. *Macromolecules* **1997**, *30* (1), 113−122.
(39) Cohen-Addad, J. P. *Macromolecules* **1989**, *22* (1), 147−151.
(40) Cohen Addad, J. P. *Prog. Nucl. Magn. Reson. Spectrosc.* **1993**, *25* (1−3), 1−316.
(41) Saalwächter, K.; Herrero, B.; López-Manchado, M. A. *Macromolecules* **2005**, *38* (9), 4040−4042.
(42) Saalwächter, K. *Macromolecules* **2005**, *38* (4), 1508−1512.
(43) Demco, D. E.; Hafner, S.; Fülber, C.; Graf, R.; Spiess, H. W. *J. Chem. Phys.* **1996**, *105* (24), 11285−11296.
(44) Schneider, M.; Gasper, L.; Demco, D. E.; Blümich, B. *J. Chem. Phys.* **1999**, *111*, 402−415.
(45) Fechete, R.; Demco, D. E.; Blümich, B. *J. Chem. Phys.* **2003**, *118*, 2411−2421.
(46) Maus, A.; Hertlein, C.; Saalwächter, K. *Macromol. Chem. Phys.* **2006**, *207*, 1150−1158.
(47) Mauri, M.; Thomann, Y.; Schneider, H.; Saalwächter, K. *Solid State NMR* **2008**, *34*, 125−141.
(48) Mora-Barrantes, I.; Malmierca, M. A.; Valentin, J. L.; Rodriguez, A.; Ibarra, L. *Soft Matter* **2012**, *8* (19), 5201−5213.
(49) Ferry, J. D. *Viscoelastic Properties of Polymers*; John Wiley & Sons, Inc.: New York, 1980.
(50) Saalwächter, K. *Rubber Chem. Technol.* **2012**, *85* (3), 350−386.
(51) Vaca Chávez, F.; Saalwächter, K. *Phys. Rev. Lett.* **2010**, *104*, 19.
(52) Che, J.; Toki, S.; Valentin, J. L.; Brasero, J.; Nimpaiboon, A.; Rong, L.; Hsiao, B. S. *Macromolecules* **2012**, *45* (16), 6491−6503.
(53) Valentín, J. L.; López, D.; Hernández, R.; Mijangos, C.; Saalwächter, K. *Macromolecules* **2009**, *42* (1), 263−272.

(54) Saalwächter, K.; Heuer, A. *Macromolecules* **2006**, *39*, 3291−3303.
(55) Valentín, J. L.; Carretero-González, J.; Mora-Barrantes, I.; Chassé, W.; Saalwächter, K. *Macromolecules* **2008**, *41* (13), 4717−4729.
(56) Baum, J.; Pines, A. *J. Am. Chem. Soc.* **1986**, *108* (24), 7447−7454.
(57) Ibarra, L.; Marcos, A.; Alzorriz, M. *Polymer* **2002**, *43*, 1649−1655.
(58) Tobolsky, A. V.; Lyons, P. F.; Hata, N. *Macromolecules* **1968**, *1* (6), 515−519.
(59) Saalwachter, K. *ChemPhysChem* **2013**, *14* (13), 3001−3014.
(60) Schneider, M.; Demco, D. E.; Blümich, B. *J. Magn. Reson.* **1999**, *140* (2), 432−441.
(61) Fechete, R.; Demco, D. E.; Blümich, B. *J. Magn. Reson.* **2004**, *169* (1), 19−26.
(62) Voda, M. A.; Demco, D. E.; Perlo, J.; Orza, R. A.; Blümich, B. *J. Magn. Reson.* **2005**, *172* (1), 98−109.
(63) Papon, A.; Saalwächter, K.; Schäler, K.; Guy, L.; Lequeux, F.; Montes, H. *Macromolecules* **2011**, *44*, 913−922.
(64) Papon, A.; Montes, H.; Lequeux, F.; Oberdisse, J.; Saalwächter, K.; Guy, L. *Soft Matter* **2012**, *8* (15), 4090−4096.
(65) Papon, A.; Montes, H.; Hanafi, M.; Lequeux, F.; Guy, L.; Saalwächter, K. *Phys. Rev. Lett.* **2012**, *108* (6), 065702.
(66) Wojtecki, R. J.; Meador, M. A.; Rowan, S. J. *Nat. Mater.* **2010**, *10*, 14−27.
(67) Hall, L. M.; Stevens, M. J.; Frischknecht, A. L. *Phys. Rev. Lett.* **2011**, *106*, 127801.
(68) Hall, L. M.; Seitz, M. E.; Winey, K. I.; Opper, K. L.; Wagener, K. B.; Stevens, M. J.; Frischknecht, A. L. *J. Am. Chem. Soc.* **2012**, *134*, 574−587.
(69) Hall, L. M.; Stevens, M. J.; Frischknecht, A. L. *Macromolecules* **2012**, *45* (19), 8097−8108.
(70) Sturniolo, S.; Saalwächter, K. *Chem. Phys. Lett.* **2011**, *516* (1−3), 106−110.
(71) Schäler, K.; Ostas, E.; Schröter, K.; Thurn-Albrecht, T.; Binder, W. H.; Saalwächter, K. *Macromolecules* **2011**, *44* (8), 2743−2754.
(72) Donnet, J.-B.; Bansal, R. C.; Wang, M.-J. *Carbon Black Science and Technology*; Marcel Dekker, Inc.: New York, 1993.
(73) Wang, M. J. *Rubber Chem. Technol.* **1998**, *71* (3), 520−589.
(74) Payne, A. R. *J. Appl. Polym. Sci.* **1962**, *6* (19), 57−63.
(75) Mora-Barrantes, I.; Rodríguez, A.; Ibarra, L.; González, L.; Valentín, J. L. *J. Mater. Chem.* **2011**, *21* (20), 7381−7392.
(76) Mujtaba, A.; Keller, M.; Ilisch, S.; Radusch, H. J.; Thurn-Albrecht, T.; Saalwächter, K.; Beiner, M. *Macromolecules* **2012**, *45* (16), 6504−6515.
(77) Heinrich, G.; Klüppel, M.; Vilgis, T. A. *Curr. Opin. Solid State Mater. Sci.* **2002**, *6* (3), 195−203.
(78) Vilgis, T. A.; Heinrich, G.; Klüppel, M. *Reinforcement of Polymer Nano-Composites*; Cambridge University Press: Cambridge, 2009.